Date: 05 March 2021

EIC Detector R&D Progress Report

Project ID:	**eRD21**
Project Name:	**EIC Background Studies and the Impact on the Interaction Region and Detector Design**
Period Reported:	1 Oct 2020—05 March 2021
Project Leaders:	Latifa Elouadrhiri and Charles Hyde
Contact Person:	Charles Hyde `chyde@odu.edu`

Project Personnel:
Vitaly Baturin* (Old Dominion University)
Pavel Degtiarenko (Thomas Jefferson National Accelerator Facility)
Latifa Elouadrhiri (Thomas Jefferson National Accelerator Facility)
Yulia Furletova (Thomas Jefferson National Accelerator Facility)
Charles Hyde (Old Dominion University)
Kyungseon Joo (University of Connecticut)
Andrey Kim* (University of Connecticut)
Alexander Kiselev (Brookhaven National Laboratory)
Frank Marhauser (Thomas Jefferson National Accelerator Facility)
Vasiliy Morozov (Thomas Jefferson National Accelerator Facility)
Christoph Montag (Brookhaven National Laboratory)
Christine Ploen* (Old Dominion University)
Marcy Stutzman (Thomas Jefferson National Accelerator Facility)
Mike Sullivan (SLAC National Accelerator Laboratory)
Mark Wiseman (Thomas Jefferson National Accelerator Facility)

* Partially supported by eRD21 project funds.

Abstract

We report on FY2021 progress of the eRD21 project on background studies. We report on synchrotron radiation, beam-gas interactions, and beam-beam interaction rates. These include comprehensive background dose rates from proton-beam plus residual-gas interactions and *ep* beam-beam interactions. Detector occupancy and synchrotron radiation studies were impacted by reduced funding in this project year. We report a synchrotron radiation study with updated electron beam optics and emittance (including halo). We have updated the beam pipe design according to the EIC project, with the exception of the 2 cm inner radius annular photon absorber in the upstream electron beam pipe and a thin gold coating on the central Be scattering chamber. We expect full synchrotron results including these critical aspects before the end of the project.

eRD21 Progress Report for FY2021

Spokespersons: Latifa Elouadrhiri and Charles Hyde

05 March 2021

Contents

1 Achievements in FY2021

1.1 Backgrounds from Beam-Gas and *ep* Interactions

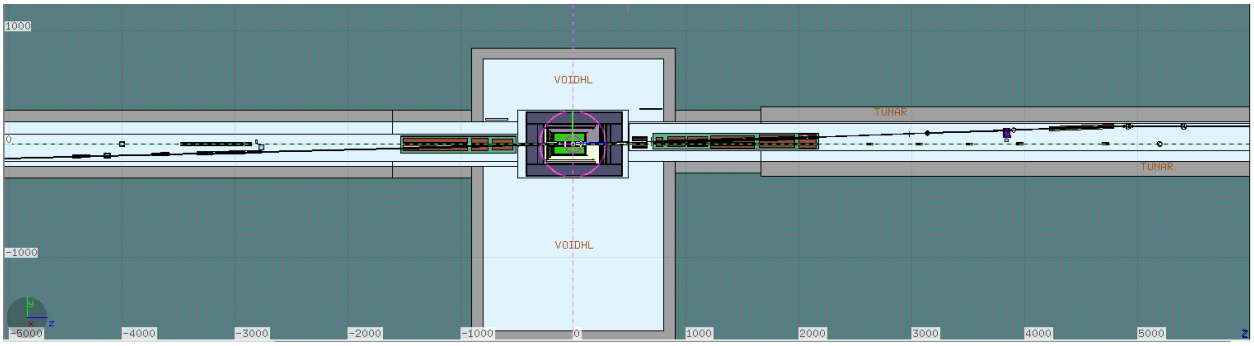

Fig. 1: FLUKA model of EIC Interaction Region 1 and detector, top view. Horizontal scale: $z = -s$ (electron beam) in cm; vertical scale (x) in floor plane is given in cm. All quads and bending magnets, as well as the central X-shaped chamber and the ion vacuum pipe are included between -50 m and $+50$ m. The ion beam enters from lower left and exits at upper right. The electron beam enters from the right travelling in $-z$ direction on the axis of the detector solenoid.

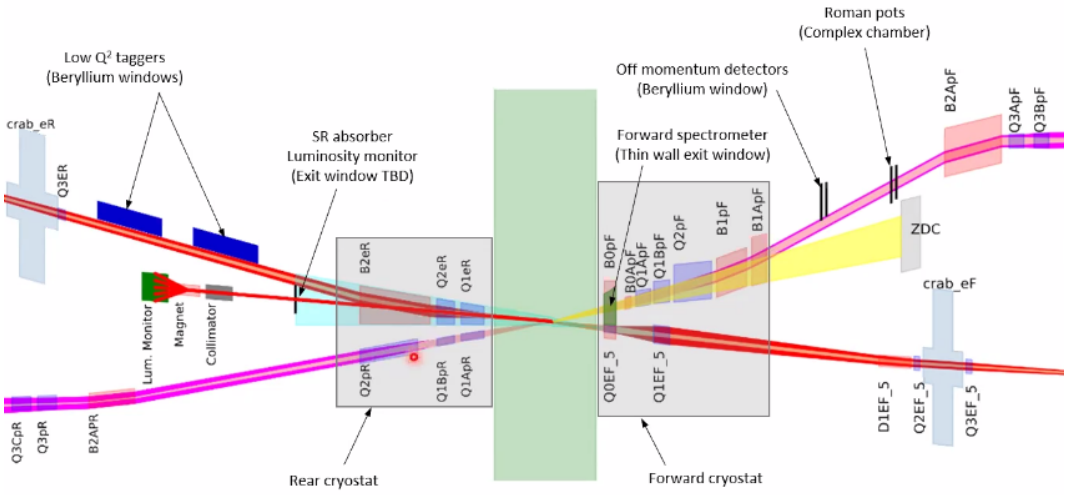

Fig. 2: Schematic view EIC beam lines with corresponding magnets in IR1.

As reported previously, we have created a FLUKA model of the the entire ion beam line at Interaction Region 1 (IR1), including all magnets ±50 m from the Interaction Point (IP), the tunnel and experimental hall walls, floor, ceilings and key elements of the detector. The FLUKA model is illustrated in Fig. 1, which can be compared with the Yellow Report schematic drawing in Fig. 2.

To achieve reasonable statistics in simulated backgrounds, we create a thin 'wire' of residual gas (95% H_2, 5%CO) along the exact beam line at an artificial pressure $P_F = 1.0$ mBar. The R&D Committee expressed some concern whether the results could reliably be scaled to the realistic residual gas pressures of 10^{-9} to 10^{-8} mBar. In Fig. 4 we illustrate the linearity of electromagnetic particle flux and neutron flux at the Si Vertex Tracker (SiVT), as a function of the 'wire' pressure

over the range $P_F = 0.1, 1.0, 10$ mBar. In addition to the central 'wire' we also compared the neutron spectra with the rest of the full beam pipe volume filled with either pure vacuum or an atmosphere of 10^{-3} mBar. The neutron spectra are indistinguishable over nine orders of magnitude.

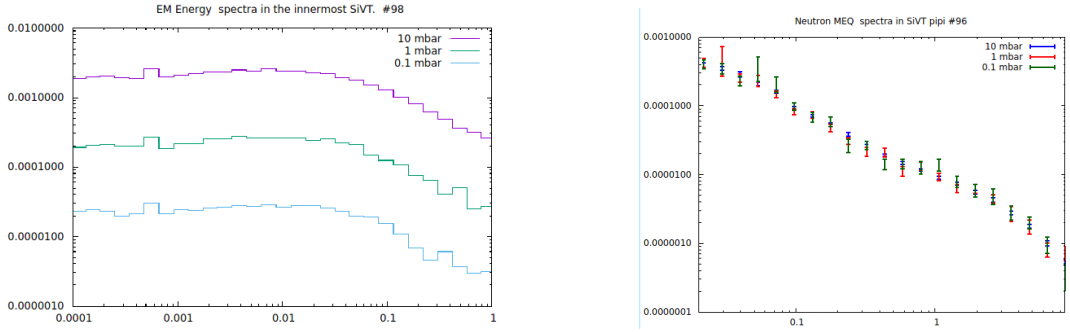

Fig. 3: Effect of the residual gas pressure in the "gas wire". **Left Plot:** Example of Electromagnetic (EM) energy fluence in the innermost SiVT barrel, (GeV/GeV/cm^2 per primary proton at at RG P_F, vertical scale) as a function of electromagnetic particle energy (GeV, horizontal scale). Three spectra are given for residual gas pressures: $P_F = 0.1$ mbar, 1 mbar, and 10 mbar. Spectra are directly proportional to the gas pressure. **Right Plot:**. Example of 1 MeV equivalent neutron fluence (Damage Function) as a function of the neutron energy in GeV (horizontal scale) per primary proton. The spectra are obtained at the same three values of P_F, but rescaled to 1 mBar.

The total hadronic background in the central region of the IR is expressed in terms of an equivalent fluence of 1 MeV neutrons in Fig. 4. The raw FLUKA fluence values, and the operational values at 1 Amp proton current and a residual gas pressure of 10^{-9} mBar are tabulated in Table 1 at critical hot spots in the detector.

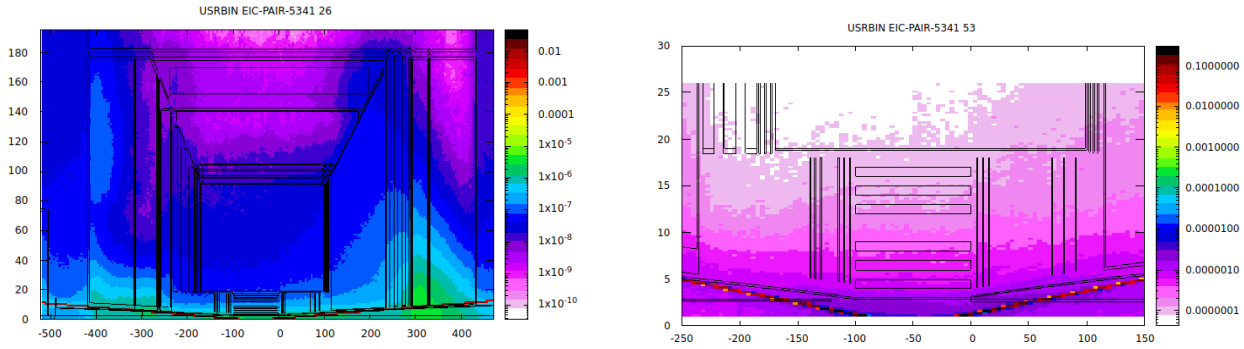

Fig. 4: Map of 1 MeV neutron equivalent fluence at the IP and surrounding detector. Horizontal scales are the z-axis of the beamline, in cm. Vertical scales are the radial coordinates, in cm. Fluence is averaged over the detector azimuth. **Left Plot:** full view of detector volume, including central tracker, endcap and barrel calorimeters. It can be seen that the calorimeters act as both sources and sinks of radiation. The ion beamline appears as a 'V' since the vertical axis integrates over the azimuth. **Right Plot:** Zoom of the central region showing the Si Vertex Tracker. The thickness of the barrel Si layers is exagerated for visual clarity. In both plots, the (different) color scale is neutrons/cm^2 per incident 275 GeV proton at a residual 'gas wire' pressure $P_F = 1$ mBar. Solenoidal field is set at 3 T. Normalized rates for $I_p = 1$ Amp stored proton current and an average residual gas pressure of $P_R = 10^{-9}$ mBar are obtained by multiplying the color scale by $(I_p/e)(P_R/P_F) = 6.25 \cdot 10^8$ protons/sec.

Table 1: Equivalent 1 MeV neutron fluence values at key locations described in columns 1–3. Column 4 are the FLUKA values from Fig. 4 of neutrons/cm^2 per 275 GeV beam proton with the arbitrary 'gas-wire' pressure $P_F = 1$ mBar. Column 5 gives the normalized fluence at the design parameters of 1 Amp proton current and a residual gas pressure $P_B = 10^{-9}$ mBar. Column 6 gives the fluence integrated over an operational year of 10^7 sec at 1 Amp. The ZDC values are discussed in Section 1.2. ZDC location a is just outside the ion beam pipe, and location b is at the center of the line-of-sight from the target: $x \approx 100$ cm.

Column	2	3	4	5	6
Detector	$z - z_{IP}$	r	Fig. 4	Fluence	Fluence
Region	(cm)	(cm)	$n/\text{cm}^2/\text{proton}$	$n/\text{cm}^2/\text{sec}$	$n/\text{cm}^2/\text{year}$
Beam Pipe	0	3	$1.5 \cdot 10^{-6}$	$9.4 \cdot 10^{3}$	$9.4 \cdot 10^{10}$
SVT	0	4	$8.0 \cdot 10^{-7}$	$5.0 \cdot 10^{3}$	$5.0 \cdot 10^{10}$
	0	6	$5.0 \cdot 10^{-7}$	$3.1 \cdot 10^{3}$	$3.1 \cdot 10^{10}$
	0	8	$3.0 \cdot 10^{-7}$	$1.9 \cdot 10^{3}$	$1.9 \cdot 10^{10}$
	0	12	$2.0 \cdot 10^{-7}$	$1.3 \cdot 10^{3}$	$1.3 \cdot 10^{10}$
	0	14	$1.5 \cdot 10^{-7}$	$9.4 \cdot 10^{2}$	$9.4 \cdot 10^{9}$
	0	16	$1.0 \cdot 10^{-7}$	$6.3 \cdot 10^{2}$	$6.3 \cdot 10^{9}$
e-EMCal	-250	10	$1.0 \cdot 10^{-6}$	$6.3 \cdot 10^{3}$	$6.3 \cdot 10^{10}$
e-EMCal	-250	20	$6.0 \cdot 10^{-7}$	$3.8 \cdot 10^{3}$	$3.8 \cdot 10^{10}$
h-EMCal	350	15	$5.0 \cdot 10^{-6}$	$3.1 \cdot 10^{4}$	$3.1 \cdot 10^{11}$
h-EMCal	350	30	$2.0 \cdot 10^{-6}$	$1.3 \cdot 10^{4}$	$1.3 \cdot 10^{11}$
ZDC	3940	a	$1.0 \cdot 10^{-5}$	$6.3 \cdot 10^{4}$	$6.3 \cdot 10^{11}$
ZDC	3940	b	$3.0 \cdot 10^{-6}$	$1.9 \cdot 10^{4}$	$1.9 \cdot 10^{11}$

1.2 Background Dose Rates from Beam-Beam *ep* Collisions

We have also implemented the physics *ep* collisions in our FLUKA model. In doing so we found that FLUKA would obtain an *ep* total inelastic cross section equal to 0 at discrete CM energies. After communication with the FLUKA team, this was corrected in the Jan 2021 FLUKA release. We are currently in communication with the FLUKA team regarding a possible anomalous energy loss when the beam is simultaneously in a magnetic field and non-zero residual gas pressure. As we added *ep* collisions, we also added the optics of the downstream ion dipole and a model Zero Degree Calorimeter (ZDC) and Roman Pot tracker. The ZDC is two meters long, with alternating equal volume layers of Tungsten and Plastic Scintillator. To examine the lateral spread of hadronic showers, the ZDC is 1 m in radius, centered on the line-of-sight from the target, and with a hole for the ion beam line.

The FLUKA results for 1 MeV equivalent neutron fluence for both beam-gas and *ep* collisions are presented in Fig. 5. The peaks in beam-gas related fluence at $z = 3100$, 3900, and 4700 cm correspond to the Roman Pot tracker, ZDC, and beam line dipole added to the simulation, respectively. The peak neutron fluence in the ZDC from beam-gas interactions is centered on the ion beam line, rather than the line-of-sight from the target. This implies that this hadronic background is dominated by primary interactions in the 10 m upstream of the ZDC, after the dipole at around 19 m downstream of the IP. In contrast, as expected, the neutron fluence generated by *ep* interactions is centered $x \approx 1$ m — the line-of-sight from the IP.

The *ep* fluence in the lower right plot of Fig. 5 is presented per hadronic inelastic *ep* scattering event. From the quasi-real photon flux, the total *ep* cross section for a $18 \otimes 275$ GeV^2 is approximately $45\,\mu$b. At a luminosity $\mathcal{L} = 10^{33}/\text{cm}^2/\text{sec} = 1000/\mu\text{b/s}$, the *ep* fluence values of Fig. 5 must be multiplied by 45,000/sec to obtain instantaneous flux. Thus the peak equivalent neutron flux in the ZDC, from physics *ep* collisions is 4,500/cm^2/sec. This is an order of magnitude less than the neutron flux at the ZDC from beam-gas interactions, obtained from the upper right plot of Fig. 5 and presented in Table 1.

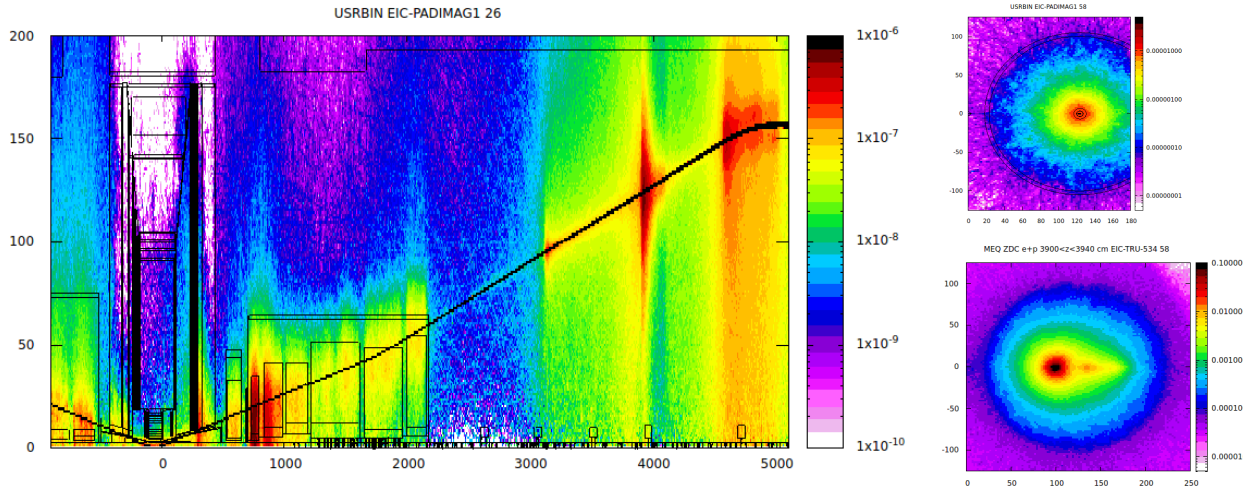

Fig. 5: **Left:** Equivalent neutron fluence in the ion downstream region from proton-beam gas interactions. The horizontal (electron beam-line) axis scale is in cm. The vertical axis is the radial coordinate is also in cm. The color scale is the neutron fluence (n/cm^2) per beam proton at a reference residual gas pressure $P_F = 1$ mBar. The fluence is averaged over azimuth, and therefore is not quantitatively accurate at the locations of off-axis ion beam-line elements. **Top Right:**. Equivalent neutron fluence from beam gas interactions displayed in the $y\,vs.x$ plane in the ZDC (at $z = 3940$ cm). **Bottom Right**: Equivalent neutron fluence from physics *ep* collisions at the IP, displayed in the $y\,vs.x$ plane in the ZDC (at $z = 3940$ cm). The color units are now n/cm^2 per inelastic *ep* collision for 18 GeV electrons incident on 275 GeV protons.

The backgrounds generated in the central detector by *ep* collisions at the IP are illustrated in Fig. 6. Normalizing to a luminosity of $10^{33}/\text{cm}^2/\text{sec}$ at $\sqrt{s} = 135$ GeV and a total *ep* cross section of $45\,\mu$b, the 1 MeV equivalent neutron rates in the SVT vary between 1800 n/cm^2/sec at the inner most radius and 110 n/cm^2/sec at the largest radius.

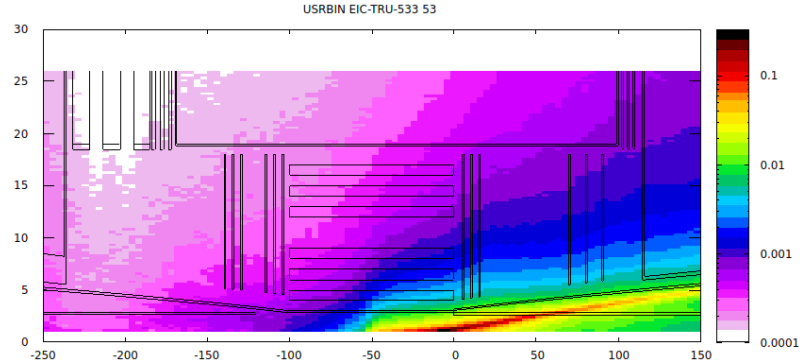

Fig. 6: 1 MeV neutron equivalent fluence (MEQ fluence) in the area of SVT caused by *ep*–collisions at $\sqrt{s} = 135$ GeV. Vertical scale-radial coordinate in cm; horizontal scale-coordinate along the electron beam line Z in cm. MEQ fluence is given in units of neutrons/cm^2 per primary *ep*–collision.

1.3 Synchrotron Radiation Background

In Nov 2020, we shifted our simulations from 18 GeV to 10 GeV electrons. The EIC Project design of the electron lattice and beam pipe continues to evolve, particularly in response to the challenge of minimizing synchrotron radiation backgrounds in the detectors. Our current simulations are based on the project lattice and beam halo estimates of October 2020.

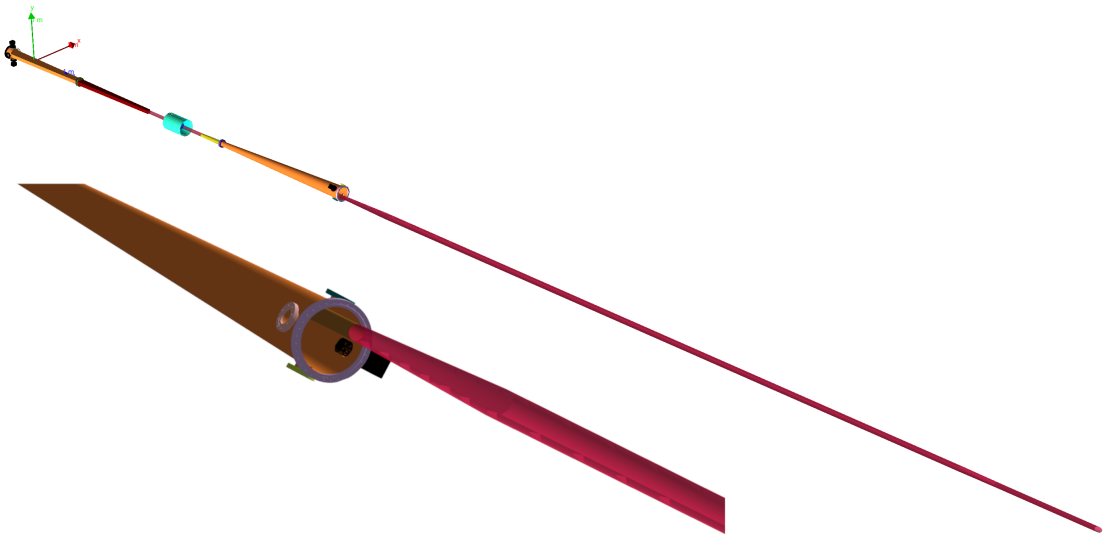

Fig. 7: Upstream electron beam pipe, central beam chamber, and Si Vertex Tracker implemented in GEANT4. The drawing displays the expansion of the pipe in the region of the quadrupoles upstream of the merger with the ion beam pipe.

In this section, we report our recent results with the SLAC code Sync_Bkg, Synchrotron photons are generated semi-analytically along the magnet lattice. In the past six months, we upgraded our GEANT4 simulation to track all X-Ray photons from their points of origin in the magnets through the IR. This enables a full study of the impact of the beam pipe, including photon absorber structures. The GEANT4 model of the beam pipe is illustrated in Fig. 7. Although difficult to see in the figure, the model includes sawtooth striations cut vertically into the inner radius of the expanded pipe to absorb, rather than rescatter, X-rays. Two key elements are not yet included in this model:

- Thin Au coating on central Be chamber still to be implemented;
- Annular photon absorber (20 mm inner radius aperture) near the pumping port in Fig. 7 still to be implemented.

The spectra of energy deposition in the Be pipe and 5 Si layers are shown in Fig. 8. The energy threshold of *e.g.* a MAPS sensor is expected at ~ 4 KeV. Thus virtually every synchrotron photon that interacts with the Si produces a hit. The energy deposition and resulting ionizing dose from synchrotron photons is illustrated in Fig. 9. Both of these figures are integrated over $1.2 \cdot 10^{11}$ beam electrons at 10 GeV (7.7 nsec at 2.5 Amp), and include estimates of the beam halo distribution. Th SVT hit rate, occupancy, and dose estimates are listed in Table 2. Both the dose rates and occupancy estimates are at least a factor of 10 too high for suitable operation. We expect a very

large reduction by the introduction of a thin $\sim 4\,\mu$m Au layer on the inside of the Be chamber, and the upstream photon absorber aperture with 2 cm inner radius. Our previous studies have demonstrated that most of the photons striking the SVT have rescattered upstream, and are not direct primary photons.

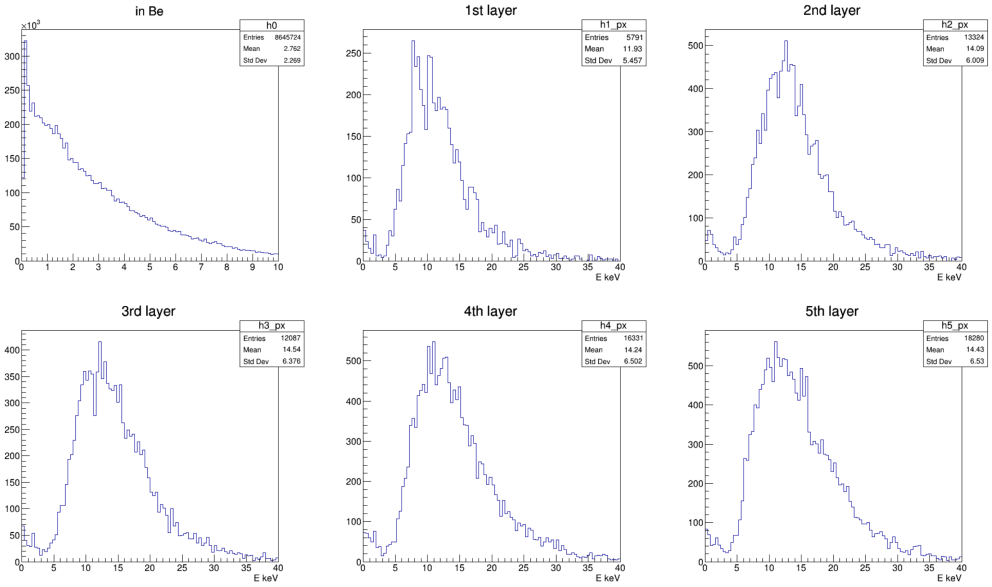

Fig. 8: Spectrum of energy deposition in Be beam pipe and five layers of SiVT, per primary synchrotron photon.

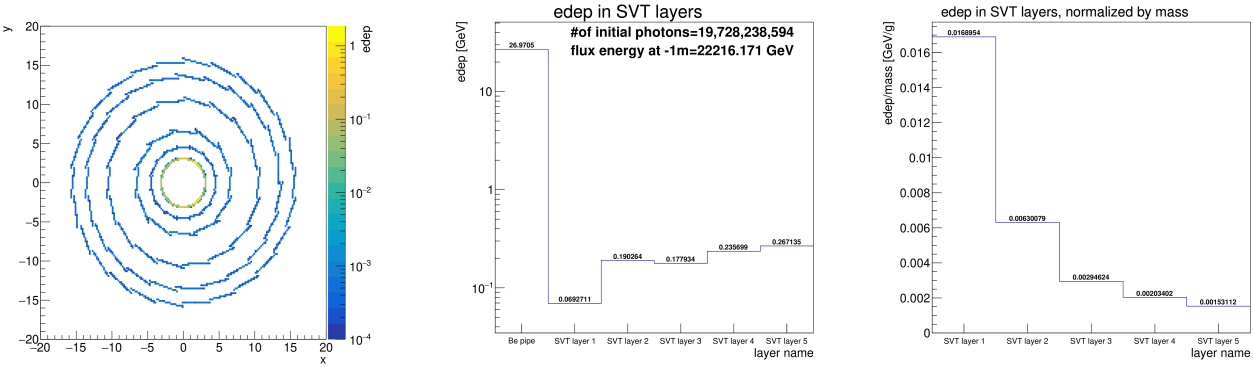

Fig. 9: **Left:** Energy deposition from synchrotron photons in the Be beam pipe ant the 5 layers of SVT. Color scale is in GeV, integrated over $1.2 \cdot 10^{11}$ incident 10 GeV electrons. At a design current of 2.5 A, this is 7.7 nsec of beam. **Center:** Synchrotron energy deposition, integrated over azimuth and z, for Be pipe and each Si layer. **Right** Synchrotron radiation dose (GeV/g) in the five Si layers, per 7.7 nsec.

Table 2: Silicon Vertex Tracker (SVT) hits and dose from synchrotron radiation

Layer #	Thickness μm	Layer Mass g	Dose GeV/g/sec	Dose Gray/sec	Dose MGray/year
1	50	4.10	$2.2 \cdot 10^6$	0.35	3.5
2	150	30.2	$8.1 \cdot 10^5$	0.13	1.3
3	150	60.4	$3.8 \cdot 10^5$	0.061	0.61
4	150	116	$2.6 \cdot 10^5$	0.042	0.42
5	150	174	$2.0 \cdot 10^5$	0.032	0.32
Layer #	Staves #	Stave Area cm^2	Hits per sec $10^{10}/cm^2/s$	Hits per readout $10^4/cm^2$ per $2\mu s$	Occupancy %
1	16	22	3.4	6.8	27
2	12	72	2.4	4.8	19
3	18	96	1.6	3.3	13
4	23	144	1.5	3.0	12
5	26	192	1.2	2.5	10

2 Ongoing Work in FY2021

2.1 Beam-Gas Interactions

We consider these studies to be nearly complete, at least as they pertain to the likely lifetime of detector components. A more detailed question relates to the likely channel occupancy of specific detector elements. This cannot be done in detail within the scope of this project. The following work-items have already started, and will be addressed during the next few months

1. Generic estimates of channel occupancy based on rates of electromagnetic energy deposition in various volumes of the model detector.

2. Background comparisons of the large ZDC described here with a more compact version *e.g.* as proposed in eRD27.

3. Evaluation of rates in the Roman Pots and Off-Momentum Detectors along the downstream ion beam line.

4. Preparation of a publication on full results.

2.2 Electron-Proton Interactions

Additional studies in process include

1. Simulations of ep collisions at $10 \otimes 275$ GeV^2. Although the CM energy is lower than reported here, the rates are likely to be higher at the maximum design luminosity $\mathcal{L} = 10^{34}/cm^2/sec$;

2. A more precise integration of the product of the quasi-real photon flux times the photo-production total cross section;

3. Compilation of ionization energy deposition, as well as neutron fluence.

2.3 Synchrotron Radiation

Work in progress:

1. Update of the electron beam pipe, as described in section 1.3;
2. Extend the model to include the downstream electron beam pipe and luminosity monitor;
3. Comparison of these results with the SYNRAD code from CERN.

3 Outlook and Requirements Beyond FY2021

At the July 2020 R&D Committee Meeting, we projected we could complete the project in one year. However, our funding for this year was reduced to 60% of our request, and our progress was impacted accordingly. Nonetheless, by the end of this fiscal year we will have an comprehensive suite of results, and we are drafting a publication. At a certain level, background studies will never be complete. Additional studies that we believe are important to pursue within the scope of EIC Project R&D include:

1. Comparison of FLUKA simulations with another framework, such as GEANT4. The programming overhead of two parallel simulation efforts was beyond the labor scope of this project.
2. Detector proposals are expected by the end of this calendar year. It would be valuable to have more detailed modeling of the specific detector layout, materials, and sensor technologies.
3. Beam-gas interactions with ion beams beyond protons. Diffractive dissociation of high energy deuterons and diffractive excitation of the Giant Dipole Resonance in medium to heavy nuclei could significantly increase the neutron yields even for the same current and residual gas pressures;
4. A full assessment of the impact of synchrotron radiation on the luminosity monitor and the low Q^2 tagger is critical, and beyond the scope of the current project.
5. The electron optics, beam line, and beam halo model all continue to evolve. The synchrotron radiation simulations need to continue, with multiple software frameworks.
6. Initial work on the dynamic vacuum resulting from synchrotron induced desorption has been done by Marcy Stutzman. This needs to continue, particularly as specific options for pump stations in the central beam pipe are developed in more detail.

4 Publications

1. V. Baturin, *et al.,* "Beam Backgrounds in the EIC", Proceedings of the Workshop on Silicon Pixel-Based Particle Vertex and Tracking Detectors Towards the US Electron Ion Collider, 02 – 04 Sept 2020. Submitted to NIM A.
2. C. Hyde, "Beam Backgrounds in the EIC", invited talk at the Workshop on Silicon Pixel-Based Particle Vertex and Tracking Detectors Towards the US Electron Ion Collider, `https://www.jlab.org/conference/SVT-EIC`, 02 – 04 Sept 2020.